Properties of Rochelle Salt

HANS MUELLER, *The George Eastman Laboratory, Massachusetts Institute of Technology*

(Received November 12, 1934)

Measurements of the dielectric, pyroelectric, optical and electro-optical properties of Rochelle salt, and a theory correlating all observations are given. The theory is based on the assumptions that all properties depend on the inner field $F=E+fP$, and that the Curie point changes with temperature. The theory explains the observed variation of the susceptibility with temperature and field strength, the anomalies of the quadratic electro-optical effect, the pyroelectric effect, the hysteresis loop, the abnormal temperature variation of the birefringence and the change of these properties if the piezoelectric deformations are prevented. It is shown that the electro-optical effect is a Kerr effect. A longitudinal Kerr effect is discovered. A small crystal represents a single Weiss region, but large crystals show a Barkhausen effect.

ROCHELLE salt is noted for its large piezoelectric effect and its anomalous dielectric behavior. The dielectric anomalies occur only for fields in the direction of the a-axis. They are very similar to the magnetic properties of ferromagnetic substances. However unlike ferromagnetism, the anomalies disappear not only above a critical temperature, but vanish also for low temperatures. There exist two Curie points, 23.7° and −18°. The piezoelectric effect varies in the same manner as the dielectric polarization. Both have sharp maxima at the Curie points and shows hysteresis and saturation at temperatures between the Curie points. Connected with the dielectric anomalies is the existence of a series of other effects, namely: the linear and quadratic electro-optic effect,[1] the electro-caloric effect,[2] the change of specific heat at the Curie points,[3] the pyroelectric effect,[4] unipolar conduction, and an abnormal temperature coefficient of the birefringence. It has been shown[5] that the rhombic hemiedric crystal structure does not change at the Curie points, but the intensity of some x-ray reflections shows an abnormal change with temperature and electric field.[6]

Two theories have been advanced to explain these properties. Cady's[7] theory takes into account the secondary effect of piezoelectricity. Kobeko and Kurtschatov[8] assume the existence of free dipoles in the crystal and develop a theory analogous to Weiss's theory of ferromagnetism. Neither theory is entirely satisfactory. Cady's theory does not explain the optical properties and Weiss's theory, as used by Kurtschatov,[8,9] cannot account for the change of the dielectric properties when the piezoelectric deformations are prevented. A satisfactory explanation of all observations can only be given by a combination of both theories.

Experimental Difficulties

Our investigations show, that it is possible to obtain reproducible data on Rochelle salt, provided the following conditions are fulfilled.

The crystal must be able to deform freely. Mechanical constraints alter radically all its properties.[10] Since good contact[11] between crystal and electrodes is required, the electrodes must be of small mechanical rigidity. Electrodes of conducting paint, graphite or metal foil[12] were found equally suitable and give the same results. The tinfoil electrode, provided it is properly attached, was found most convenient. The electrodes must cover the entire face of the crystal. Uncovered edges are a source of constraining forces for the interior part of the crystal. The

[1] F. Pockels, Göttinger Nachrichten, 1895.
[2] P. Kobeko and I. Kurtschatov, Zeits. f. Physik **66**, 192 (1930).
[3] P. Kobeko and J. Nelidov, Phys. Zeits. d. Sow. **1**, 382 (1932).
[4] J. Valasek, Phys. Rev. **17**, 475 (1921); **20**, 639 (1922); **19**, 478, 529 (1922); **24**, 560 (1924).
[5] H. M. Krutter and B. E. Warren, Phys. Rev. **43**, 500 (1933).
[6] H. Staub, Helv. Phys. Acta. **7**, 1, 480 (1934).
[7] W. G. Cady, Phys. Rev. **33**, 278 (1929).
[8] I. B. Kurtschatov, Seignette—*Electricity*, Monograph, 1933.
[9] B. and I. Kurtschatov, Phys. Zeits. d. Sow. **3**, 321 (1933).
[10] C. B. Sawyer and C. H. Tower, Phys. Rev. **35**, 269 (1930).
[11] Busch, Helv. Phys. Acta **6**, 315 (1933).
[12] Electrodes of evaporated silver (A. Zeleny and J. Valasek, Phys. Rev. **46**, 450 (1934)) were found to be unsatisfactory since the crystal effloresces in the vacuum.

crystal is either suspended on strips of tinfoil attached to the electrodes, or supported on knife edges along the lines for which the piezoelectric displacements vanish.

The temperature must be accurately controlled. The dielectric and optical measurements provide very accurate means to ascertain that the entire crystal has the same temperature as the bath. It was found necessary to wait more than two hours before temperature equilibrium was reached. The temperature is measured with two or more separate thermocouples, one of which is attached to one electrode, and a type K potentiometer.

Surface conductivity is practically eliminated by annealing the crystal for several hours at 45°, and drying it for about 20 minutes over phosphorous pentoxide. Dehydration of the surface layer must be avoided. For a properly annealed and dried crystal the electric strength is more than 20 kv/cm.

The influence of the electrolytic conduction is minimized by the use of a.c. methods. We have verified[11] that the dielectric properties are the same for frequencies up to 5000 cycles.

In measurements with d.c. voltages the complications due to conductivity are avoided by making all observations immediately after the voltage is applied, and by grounding both electrodes immediately afterwards. The next observation is made with the field reversed. After a few preliminary trials it is possible to set the measuring device very close to the correct setting and readings can be made before the field has appreciably changed.

The Crystals

All crystals were grown, cut, and some also foiled by the Brush Development Company. The uniformity of the results gathered on more than twenty different crystals testifies for the purity of the material. In Table I we give the dimensions of the crystals which were used in the final measurements.

Table I. *Length in direction* (mm).

No.	1	2	3	4	5	6	7	8
a	3.1	2	2.2	25	25	8.1	20	34
b	60	37	55	1.5	25	13.8	50	10
c	100	56	31	25	1.5	29.6	90	10

Experimental Methods

Dielectric measurements were performed with the following methods:

(a) Bridge measurements with a General Radio capacitance bridge, using 1000 cycle a.c. of a tuning fork oscillator. The bridge output is amplified with a two stage resistance coupled amplifier. The substitution method was used. The crystals are suspended in sealed glass tubes, which are immersed in the bath whose temperature is controlled by a mercury regulator.

(b) Determination of the a.c. capacity while the crystal is under the influence of a d.c. voltage. For this purpose the bridge arm is modified, as shown in Fig. 1.

(c) The same arrangement in Fig. 1 is connected in parallel with the condenser of an audio-frequency oscillator. The change of capacitance with field strength produces a frequency change of the oscillator.[13]

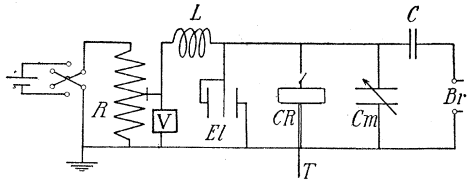

Fig. 1. Modified bridge arm. V voltmeter, El electrometer, CR crystal condenser, Cm measuring condenser, $L=60$ henry, $C=2$ mf.

(d) Investigation with the cathode-ray oscillograph. Sawyer and Tower's[10] method is improved by the use of the arrangement shown in Fig. 2. The resistance R serves to correct for the power loss in the crystal. The cathode-ray oscillograph uses the R.C.A. tube 905. Measurements with 500 cycles are found to be more reliable than with 60 cycles.

Optical and Electro-Optical Investigations

All optical investigations were made with monochromatic light of $\lambda=5461$A furnished by a Hg arc and a filter. The optical system consists of a polarizing nicol, a Babinet compensator, a low power microscope with the analyzing nicol between ocular and objective and a system of

[13] Demonstrated at the meeting of the A. A. P. T., December, 1933.

lenses and stops to produce a parallel pencil of light. The compensator permits measurements of a change of optical path of $1/150\lambda$. The light passes through the crystal in the direction of one of the axes and is polarized at 45° to the other two axes. The crystal is mounted in a brass tube which passes horizontally through the temperature bath. The tube is closed by two sets of plane parallel windows. The orientation of the crystal is adjusted by moving the whole bath, which is mounted on a movable platform. In making the adjustment we made use of the fact that the linear electro-optical effect must vanish if the light passes in the direction of the b or c axes. The surfaces of the crystals, where the light enters and leaves, are polished and parallel. For measurements above 40° it is necessary to protect the polished faces with a cover glass, attached with balsam in xylene, otherwise the surface soon becomes opaque due to efflorescence. The voltage is furnished by a kenotron outfit, and measured with a galvanometer and high resistances.

Pyroelectric Measurements

This experiment required a particularly careful mounting of the crystal. Two rings of fused quartz hold it in a small brass tube in the center of a large well stirred temperature bath. All leads are shielded and insulated with quartz capillaries. The temperature is changed in steps of about 2° and, after every change, temperature equilibrium is attained. The method of Gaugain[14] was used for qualitative observations, but for quantitative measurements the compensation method of Ackermann[15] was employed. We constructed a quartz insulated Harms-condenser with a capacity of 1158 mmf and used an Edelmann-Lutz string electrometer at a sensitivity of 0.01 volt per scale division.

Evaluations and Correction

The dielectric constant in the a direction was calculated by using for the geometrical capacitance $C_g = A/4\pi t$. Busch[11] has used Kirchhoff's correction for the edge effect, but if one takes into account the large ratio between the dielectric constant in the a direction and the constants in the b and c directions, one realizes that this edge effect is negligible. For the same reason the Chaumont correction for the Kerr effect can be omitted. We have varied the ratio of electrode area to thickness by a factor 10 without discovering any influence of the edge effects.

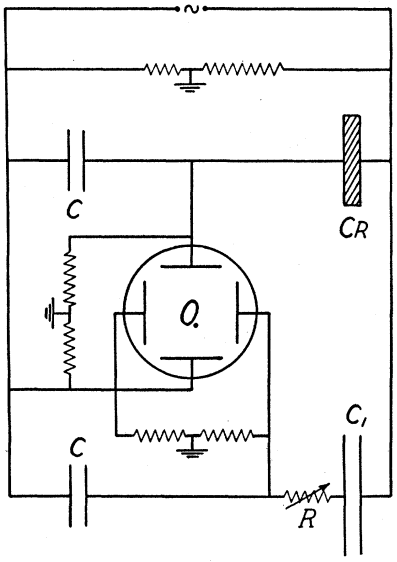

FIG. 2. Oscillograph connections. O oscillograph, $C = 0.03$ mf, $C' = 0.6$ mf, Cr crystal.

In the range where the polarization P is not proportional to the field E, we assume that the a.c. measurements give $\kappa_E = \partial P/\partial E$ for the value of E corresponding to the superposed d.c. voltage.

The cathode-ray oscillograms are evaluated with the help of calibration curves. From Fig. 2 it is evident that the oscillograms are not true $P(E)$ curves. To construct these curves the photographs were projected on cross-section paper and the necessary corrections applied.

The optical and electro-optical measurements give $(n_a - n_b)/\lambda$, etc. The thickness of the crystals made it necessary to carry out all observations on an interference line of high order. The order number S was not determined. Its value can be estimated by using Valasek's[4] values of the indices of refraction n_a (of light, whose electric vector oscillates in the a direction), n_b and n_c. Though we are not able to give the absolute values of the birefringence, we can measure

[14] W. Voigt, *Lehrbuch der Kristallphysik*, p. 239.
[15] Ackermann, Ann. d. Physik **46**, 197 (1915).

accurately its change with temperature and electric field. For the purpose of our investigation this is sufficient. The influence of the optical activity of Rochelle salt can be neglected.

Theory

We intend to discuss the molecular theory of Rochelle salt in another paper. For the purpose of discussing the experimental results, it is sufficient to consider a phenomenological theory. This theory is based on H. A. Lorentz's result that the electric field acting on the molecules is

$$F=E+fP. \tag{1}$$

Since Rochelle salt is orthorhombic the factor f differs from Lorentz's value $4\pi/3$ and depends on the direction of the field. Since for ordinary dielectrics F and E are proportional, we assume that the dielectric polarization, the piezoelectric deformation y_z, the electro-optical effects and the change of scattering of x-rays depend on F in the same manner as they depend on E in normal dielectrics. We postulate therefore

$$y_z=\delta_{14}F. \tag{2}$$

The available data[16] are not sufficient to decide whether a term in F^3 should be introduced in (2). Since in the important temperature range fP is much larger than E, this postulate agrees with the observed proportionality of y_z with P. The dielectric polarization is given by

$$P=\alpha F-\beta F^3. \tag{3}$$

The linear term is the result of four effects

$$\alpha=\alpha_1+\alpha_2+\alpha_3+\alpha_4,$$

where α_1 is the optical polarizability, α_2 is due to the displacement of ions in the lattice, $\alpha_3=e_{14}\delta_{14}$ is due to the piezoelectric back polarization[16] $e_{14}y_z$ and α_4 gives the contribution of dipoles. In a finite plate α_3 depends on the geometrical dimensions of the crystal, and vanishes if the deformations are prevented. α_3 and α_4 are responsible for a marked temperature dependence of α.

The term βF^3 may be due to the existence of a cubic term in (2) or it is due to the orientation of dipoles. The present data do not require the introduction of higher powers of F in (3).

The quadratic electro-optical effect is proportional to F^2. If Δ_a designates the change of $(n_b-n_c)/\lambda$ produced by an electric field, we assume

$$\Delta_a=\rho_aF^2;\quad \Delta_b=\rho_bF^2;\quad \Delta_c=\rho_cF^2. \tag{4}$$

This definition requires

$$\rho_a+\rho_b+\rho_c=0. \tag{5}$$

Since Δ_a represents a change of the polarization of light passing through the crystal in the direction of the applied field, we shall call it a "longitudinal Kerr effect." The "longitudinal Kerr constant" ρ_a can be calculated with the help of (5) from the "transversal Kerr constants" ρ_b and ρ_c.

From (1) and (3) we get

$$E=(1-\alpha f)F+\beta fF^3.$$

The Curie points are the temperatures where $\alpha f=1$. We introduce therefore as "Curie temperature" Θ

$$\Theta=\alpha fT \tag{6}$$

and get the fundamental equation

$$E=(1-\Theta/T)F+\beta fF^3. \tag{7}$$

The Curie temperature Θ is a function of the temperature. The dielectric properties at the temperature T are analogous to the magnetic properties of a ferromagnetic substance whose Curie point is at the temperature $\Theta(T)$. While the concept of a variable Curie point, or Curie temperature, is new, the ideas on which this concept is based are identical with those of Kurtschatov, Bernal and Fowler,[17] and of Debye. (Theory of the dielectric properties of liquids with polar molecules.)

The experimental Curie points T_c, defined as the temperatures where the transition from the normal to the "ferro"-dielectric state occurs, are the solutions of the equation $\Theta(T)=T$.

It is convenient to assume that within small temperature ranges Θ is a linear function of the

[16] S. Bloomenthal, Physics **4**, 172 (1933).

[17] Bernal and Fowler, J. Chem. Phys. **1**, 515 (1933).

absolute temperature T. For temperatures t (centigrades) near the Curie points we can therefore write

$$T-\Theta=\gamma(t-t_c), \tag{8}$$

where $(1-\gamma)$ is the slope of $\Theta(T)$ at the Curie point. If $T>\Theta$ the dielectric behavior is normal; if $T<\Theta$ the anomalies occur. We consider the two cases separately.

$T < \Theta$

For very small fields E the dielectric susceptibility κ_0 follows a law similar to the Curie-Weiss law for ferromagnetism

$$\frac{1}{\kappa_0}=\frac{f}{\Theta}(T-\Theta).$$

Near the Curie point this leads to the approximation

$$\frac{1}{\kappa_0}=\frac{f\gamma}{T_c}(t-t_c)=\frac{t-t_c}{C}. \tag{9}$$

The Kerr effect for small fields is

$$\Delta=\frac{\rho T^2}{(T-\Theta)^2}E^2=KE^2\cong\frac{\rho T_c{}^2}{\gamma^2(t-t_c)^2}E^2, \tag{10}$$

where the last expression holds only near the Curie point. K is Kerr's constant as usually defined. Eqs. (9) and (10) are limiting laws for $E\to 0$. The larger $(T-\Theta)$ the wider their range of validity.

In the range where the term $\beta f F^3$ is small, but not negligible, we can make the development

$$F=\frac{1}{1-\Theta/T}E-\frac{\beta f}{(1-\Theta/T)^4}E^3.$$

This leads to

$$\kappa_E=\kappa_0(1-GE^2) \tag{11}$$

with

$$G=\frac{3\beta f}{(\Theta/T)(1-\Theta/T)^3}$$

or near the Curie point

$$\left(\frac{1}{G}\right)^{\frac{1}{3}}=\frac{\gamma}{T_c}\left(\frac{1}{3\beta f}\right)^{\frac{1}{3}}(t-t_c)=g(t-t_c). \tag{12}$$

For the Kerr effect the second approximation gives

$$\Delta=KE^2\left[1-\frac{2\beta f}{(1-T/\Theta)^3}E^2\right]. \tag{13}$$

The range of validity of (11) and (13) is very limited. They hold only for not very large fields and temperatures not too near the Curie point. At the Curie point we get $\kappa_0=\infty$

$$\kappa_E=\frac{1}{f}\left[\frac{1}{3}\left(\frac{1}{\beta f E^2}\right)^{\frac{1}{3}}-1\right]$$

and

$$\Delta=\rho(E/\beta f)^{\frac{3}{2}}. \tag{14}$$

The best experimental results are obtained at temperatures slightly above the Curie point, where the second approximation holds for small fields only. Hence it is important to develop general formulas which hold for large fields. Using (7) and (4) we get for the Kerr effect

$$E/(\Delta)^{\frac{1}{2}}=R(t-t_c)+Q\Delta, \tag{15}$$

where

$$R=\frac{\gamma}{T_c\rho^{\frac{1}{2}}}=\frac{1}{(K)^{\frac{1}{2}}}\frac{1}{(t-t_c)}, \tag{16}$$

$$Q=\beta f/\rho^{\frac{3}{2}}. \tag{17}$$

A similar formula can be derived for the susceptibilities. We introduce

$$X=\frac{(\kappa_0-\kappa_E)f^2}{(1+f\kappa_0)(1+f\kappa_E)}.$$

Near the Curie point κ_0 and κ_E are very large, and hence X is given with sufficient accuracy by

$$X=(\kappa_0-\kappa_E)/\kappa_0\kappa_E. \tag{18}$$

Eq. (7) leads then to

$$E/(X)^{\frac{1}{2}}=M(t-t_c)+NX, \tag{19}$$

where

$$M=\gamma/fT_c(3\beta)^{\frac{1}{2}};\quad N=1/3f^2(3\beta)^{\frac{1}{2}}. \tag{20}$$

$T < \Theta$

In this temperature range we get a spontaneous polarization P_0. With $E=0$ Eq. (7) gives

$$P_0{}^2=(F_0/f)^2=(1/\beta f^3 T)(\Theta-T), \tag{21}$$

where F_0 is the spontaneous inner field. Near the Curie point we get

$$P_0^2=(\gamma/\beta f^3 T_c)(t_c-t)=h(t_c-t). \qquad (21')$$

This spontaneous polarization, since it depends on temperature, manifests itself in the same way as an ordinary pyroelectric effect. The crystallographic symmetry of Rochelle salt does not permit an ordinary pyroelectric effect. Its apparent pyroelectricity is due to this spontaneous polarization. The existence of this effect is therefore no violation of Neumann's principle. The direction of P_0 is parallel to the a-axis, "the direction of easy polarization" but the sign of P_0 is not determined by the theory.

The spontaneous field produces a spontaneous Kerr effect

$$\Delta_0=(\rho/\beta f T)(\Theta-T) \qquad (22)$$

or, near the Curie point

$$\Delta_0=(\rho\gamma/\beta f T_c)(t_c-t)=\nu(t_c-t). \qquad (22')$$

This effect is superposed upon the normal change of birefringence with temperature and produces an anomalous temperature variation of the birefringence.

The spontaneous field F_0 is also responsible for the temperature dependence of the scattering of x-rays. The energy necessary to produce P_0 leads to a change of the specific heat.

The range of spontaneous polarization extends from $-18°$ to $+23.7°$. The difference $\Theta-T$ has a maximum at about 0°, where it is about 10°. Consequently the dielectric properties of Rochelle salt are not comparable with the magnetic properties of iron at room temperature, but they are analogous to the ferromagnetic properties near the Curie point. This fact justifies the use of Eq. (7) for the "ferro-electric" temperature range.

The susceptibility for small fields ($E=0$, $F=F_0$) is given by

$$\kappa_0=T/2f(\Theta-T)-1/f.$$

Near the Curie points this leads again, by neglecting small terms, to a law similar to the Curie-Weiss law

$$\frac{1}{\kappa_0}=\frac{2f\gamma}{T_c}(t_c-t)=2\frac{t_c-t}{C}. \qquad (23)$$

The Kerr effect for small fields dE is

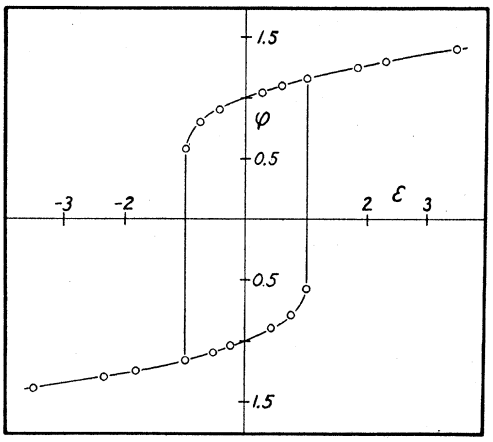

FIG. 3. Theoretical hysteresis curve.

$$d\Delta=\frac{\rho}{\pm[(\beta f/T)(\Theta-T)]^{\frac{1}{2}}}dE;$$

hence the quadratic electro-optical effect is in first approximation proportional to the absolute value of the applied field. Near the Curie points we get

$$\Delta=[L/(t_c-t)]^{\frac{1}{2}}|E|, \qquad (24)$$

where $L=\rho^2 T_c/\gamma\beta f$.

For larger fields the theory gives a hysteresis loop of the form shown in Fig. 3. In this diagram we have plotted $\varphi=F/F_0$ versus $\epsilon=E/E_c$ where E_c is the coercive field

$$E_c=\frac{2}{3T}\frac{1}{(3\beta f T)^{\frac{1}{2}}}(\Theta-T)^{\frac{3}{2}}. \qquad (25)$$

Near the Curie point we have

$$E_c=\tfrac{2}{3}g^{\frac{1}{2}}(t_c-t)^{\frac{3}{2}}. \qquad (26)$$

The "reduced" hysteresis loop in Fig. 3 is the same for all temperatures $T<\Theta$. Since we have always $P\gg E$ the loop for $P(E)$ is similar to the $F(E)$ loop. The remanent polarization is identical with the spontaneous polarization P_0.

In the experiments hysteresis loops are observed, but they do not show the large Barkhausen jumps predicted by the theory. We believe that this is due to the interaction between polarization and piezoelectric deformation. The deformation cannot change with infinite velocity. Hence the loop is smoothed out in a way which

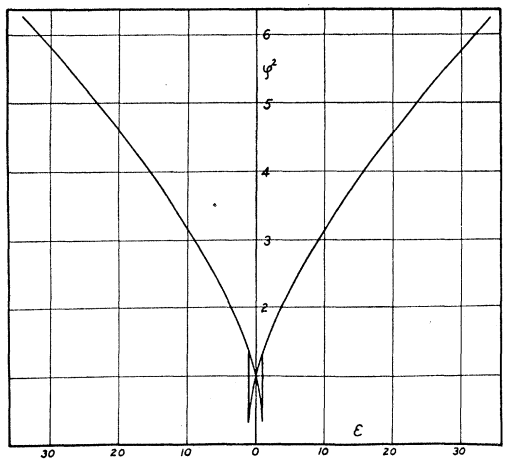

FIG. 4. Kerr effect between the Curie points. Theoretical curve.

depends on the elastic properties of the crystal. The formulas for P_0 and E_c can therefore not be exactly verified, but they give the correct order of magnitude and the temperature dependence of the height and width of the loops.

For fields large compared with E_c we have by no means saturation as is usually stated. Since we are always near the Curie point, we must expect a further increase of P with E. Also, the Kerr effect does not show saturation. Fig. 4, which has been constructed by using Eq. 7, shows how this effect should vary with the applied field for any temperature between the Curie points. For small fields we get a quadratic hysteresis loop. For large fields the Kerr effect is nearly proportional to the absolute value of the applied field.[18]

We wish to develop here the theory only as far as it has a relation to our experimental work. There are no difficulties in applying it to the electro-caloric effect, the change of specific heat, the change of x-ray scattering, the linear electro-optical and the piezoelectric effect.

[18] Previously the author (Phys. Rev. **40**, 1051 (1932)) has proposed another explanation for this curious behavior of a quadratic effect. While the fundamental idea is the same as in this paper, the mathematical formulation cannot be accepted. The older theory requires an increase of the slope of the $\Delta(E)$ curves with increasing values of $(\theta-T)$ and of E. The present theory gives according to (24) a smaller Kerr effect for larger values of $(\theta-T)$ and a slightly decreasing slope for increasing field strengths. The experiments definitely support the conclusions of the present theory.

Eighteen of the above equations are subject to experimental verification. They are used to determine the values of C, g, R, Q, M, N, h, v and L. Near the Curie point these 9 constants depend only on the values of γ, f, β and ρ. We have therefore a series of possibilities to cross check our theory by the following relations between the experimental constants:

$$g=(M^2/C)^{\frac{1}{3}}, \quad (27) \qquad v=R/Q, \quad (30)$$

$$Q=\tfrac{1}{3}(R/g)^3, \quad (28) \qquad L=1/RQ, \quad (31)$$

$$N=\tfrac{1}{3}CM, \quad (29) \qquad h=9NM. \quad (32)$$

These six relations reduce the number of independent quantities to three and we are therefore not able to determine all four quantities γ, f, β and ρ but only the combinations

$$f\gamma=T_c/C. \ (33)\ ; \ \beta f^4=1/27N^2. \ (34)\ ; \ \rho f^2=v/h. \ (35)$$

These equations hold for both Curie points. The value of γ is positive for the upper, and negative for the lower Curie point. ρ and β will vary with temperature, but f is a constant.

EXPERIMENTAL RESULTS

All data[19] are given in c.g.s.e. units. The error limits are estimated from the variation of the data on different crystals. Data on the same crystal are reproducible and give much smaller error limits.

$T > \Theta$

The susceptibility κ_0. Method: a.c. bridge. Crystals 1, 2 and 3 were used for the temperature range from $-180°$ to $-15°$ and $+20°$ to $+50°$. Fig. 5 gives the reciprocal susceptibility *versus* temperature of two crystals above the upper Curie point. We call attention to the analogy between this curve and the curves for the paramagnetic susceptibility of iron and nickel[20] above the Curie point. Between 34° and 50° the

[19] In making the measurements I have been assisted by a number of students. Credit must be given to Miss Lucy M. Groat, who performed a large part of the optical and electro-optical determinations, to Mr. J. E. Forbes, for the dielectric measurements with the a.c. bridge, to Mr. E. B. Bradford for the investigations with the cathode-ray oscillograph and to Mr. L. Tarnopol for the investigation of the pyroelectric effect.

[20] Weiss and Foëx, Arch. de Geneve **31**, 89 (1911).

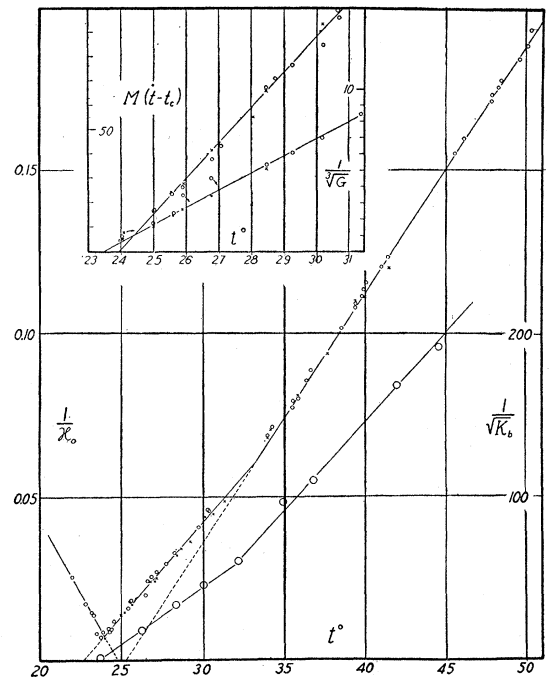

FIG. 5. Curie-Weiss law for $1/\kappa_0$, (o crystal 1, x crystal 2) and for $K_b^{-\frac{1}{3}}$ (crystal 6). Inset: $G^{-\frac{1}{3}}$ and $M(t-t_c)$. (o crystal 2, x crystal 3).

measurements on all three crystals follow very accurately the law

$$1/\kappa_0=(1/c_i)(T-T_i) \qquad (36)$$

with $c_1=136\pm0.5$ and $T_1=273+25.3\pm0.05$. Between 25° and 32° the results can be represented by the same law, but with

$$c_2=178\pm5 \qquad T_2=273+23\pm0.5.$$

The Curie point is at $23.67\pm0.03°$. In view of the great difficulties in getting reproducible results for temperatures very near the Curie point, we feel justified in assuming $T_2=T_c$ and $C=c_2$.

Since the low temperatures could not always be kept constant for a sufficiently long period the data in Fig. 6 are less accurate. As was first noticed by Valasek, the susceptibility can again, within small temperature ranges, be represented by the law (36) but this is more a matter of convenience than of necessity. We get

from	$-18°$ to	$-28°$	$c_3=-93.8=C'$	$T_3=273-17.9=T_c'$
"	-28 to	-42	$c_4=-68.5$	$T_4=273-20.6$
"	-42 to	-80	$c_5=-47.9$	$T_5=273-27.1$
"	-100 to	-140	$c_6=-80.6$	$T_6=273+16.6$

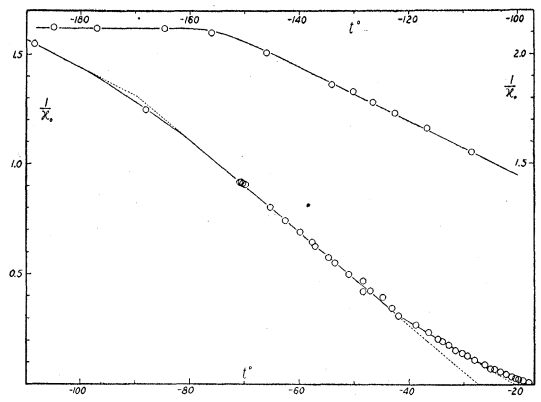

FIG. 6. Reciprocal susceptibility of Rochelle salt below $-18°$.

Below $-160°$ the dielectric constant is independent of temperature.

The experimental law (37) is compatible with Eq. (9) provided

$$\Theta=T/[1+(1/c_if)(T-T_i)]. \qquad (37)$$

The large values of c_i justify our assumption (8). Eq. (37) will serve to determine $\Theta(T)$.

Crystals 4 and 5 were used to measure the dielectric constants ϵ in the b and c direction. Since the corrections for the edge effect are here very large no accurate values can be given. For 25° we find approximately $\epsilon_b=10$, $\epsilon_c=9.6$. Both constants show a definite increase with temperature. We find $(1/\epsilon_b)(d\epsilon_b/dt)=0.007$ and $(1/\epsilon_c)\times(d\epsilon_c/dt)=0.003$. At the Curie points no abnormal change is observed.

The susceptibility κ_E. Method: a.c. bridge with bridge arm in Fig. 1. Crystals 2 and 3 were measured between 22° and 35°. Above 32° no change of κ with field was observed. Fig. 7 shows that Eq. (11) is verified. From the initial slopes of these curves we find $G^{-1/3}$ (see Fig. 5) and verify the theoretical law (12). Fig. 5 gives

$$g=1.05\pm0.02.$$

Verification of (11) has also been given by Kurtschatov[8] but we cannot agree with his conclusion that the deviations from this law require the introduction of higher powers of F in Eq. (7). The deviations are due to the fact that (11) is an approximation. Eq. (7) can be verified by testing the validity of the general law (19). This is done

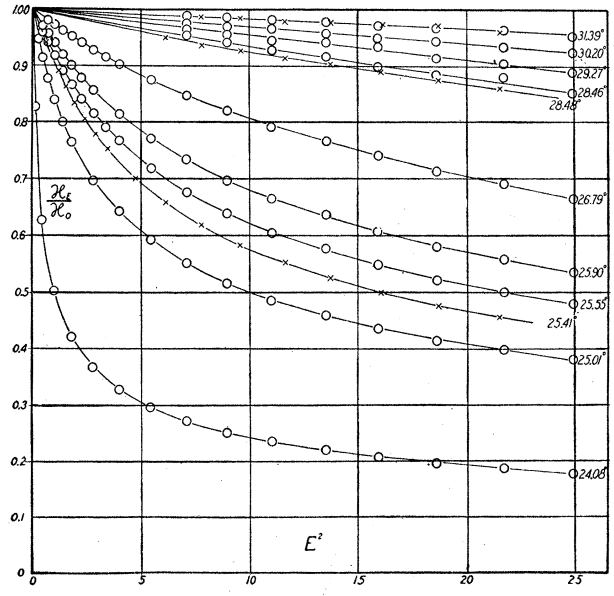

FIG. 7. Change of the susceptibility with field intensity; o crystal 2; x crystal 3.

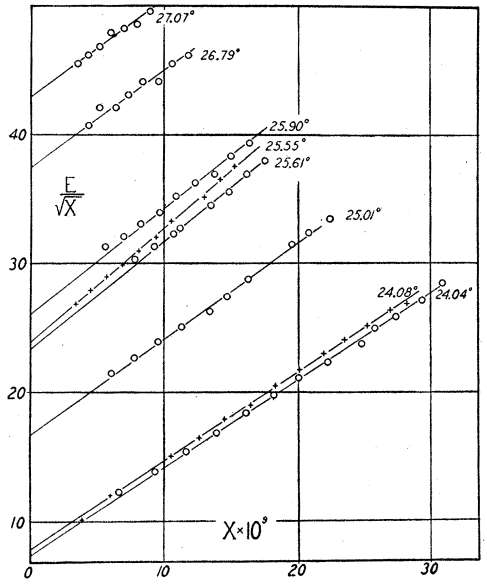

FIG. 8. $E/X^{\frac{1}{2}}$ *versus* $X=(\kappa_0-\kappa_E)/(\kappa_0/\kappa_E)$.

in Fig. 8. The slope of the straight line varies slightly, but does not show any regular change with temperature. Its average value is

$$N=800\pm80.$$

The ordinate for $X=0$ must be proportional to $(t-t_c)$. This is verified in Fig. 5, which gives $t_c=23.75$ and

$$M=13.5\pm0.4.$$

Observations with the Cathode-Ray Oscillograph

The oscillograms do not give accurate determinations, but they are a convenient method to demonstrate and verify the previous observations. The photographs in Fig. 9 illustrate the change of the $P(E)$ curves as one approaches the upper Curie point. From these photographs the $Q(E)$ curves are constructed in Fig. 10, Q is the charge per cm². Since $P\gg E$ we can approximate $Q=F/f$ and get from (7)

$$E=[(t-t_c)/C]Q+\beta f^4Q^3. \qquad (38)$$

The curves in Fig. 10 are drawn according to this law, with the values $t_c=23°$, $C=170$, $\beta f^4=1.10^{-7}$. Curves similar to Fig. 9 are obtained

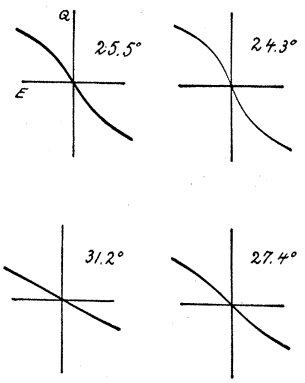

FIG. 9. Photographs of cathode-ray oscillograms showing the dependence of polarization on the field above the Curie point.

below the lower Curie point. (See Fig. 16.) The oscillogram as well as the measurements of κ_E give the same results if the direction of E is reversed.

The Quadratic Electro-Optical Effect

Crystal 7 was investigated for light passing in the c direction, and crystal 6 was used in all three orientations. Preliminary investigations, using six other crystals, showed that the effect is reproducible, provided the effect of conduction

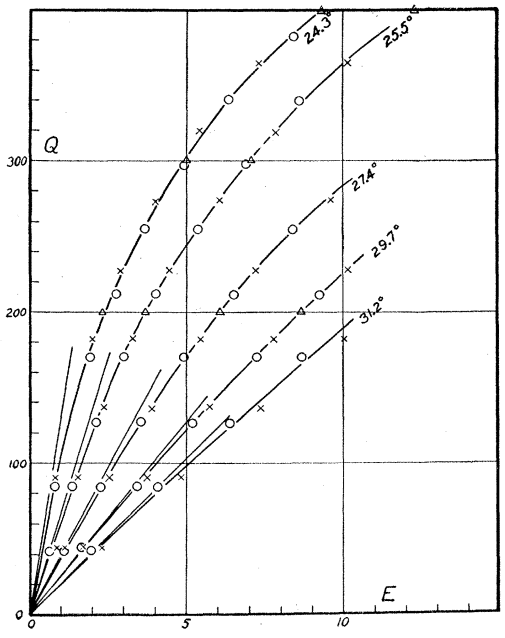

FIG. 10. Dependence of the induced charge Q on the applied field E for temperatures above the Curie point. o, x observed values for $\pm E$, Δ calculated.

is eliminated. The Kerr effect was observed to exist in the temperature range from $-30°$ to $+45°$ but measurements were made only above 0°. Comparison of the transversal effects, made on the same crystal, gave for all temperatures and fields a constant ratio

$$\Delta_b/\Delta_c=\rho_b/\rho_c=-95/70.$$

In both directions the electric field produces an increase of the natural birefringence. Since $n_a>n_b>n_c$ we must consider ρ_b as a negative, ρ_c as a positive quantity. According to (5) there exists therefore for Rochelle salt a longitudinal Kerr effect

$$\rho_a=-(\rho_b+\rho_c)=(25/70)\rho_c.$$

The longitudinal effect is again an increase of birefringence. The existence, direction and magnitude of this longitudinal effect was directly verified in a separate experiment, in which the light passed through pin holes in the electrodes. Only observations at room temperature were made. At this temperature the effect is nearly proportional to the absolute value of the field. The result of this experiment casts serious doubt

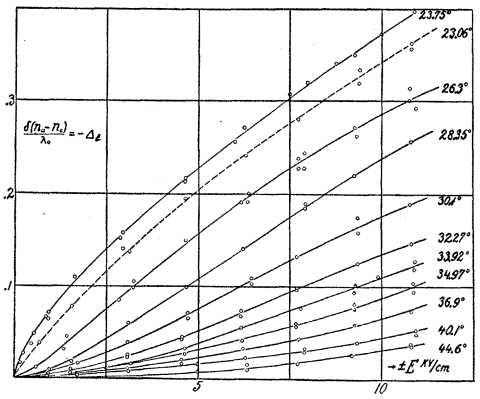

FIG. 11. The Kerr effect in Rochelle salt for light passing in the direction of the b axis at temperatures above the upper Curie point (crystal 6).

upon the interpretation of a similar experiment of Valasek.[4] We come to the conclusion that Valasek observed not the linear, but the longitudinal quadratic electro-optical effect. Our observations contradict his statement that the change of birefringence is reversed with reversal of the field. It is linear, but it cannot be reversed.

Fig. 11 gives the observations in the b direction of crystal 6. Above 40° the Kerr effect is normal and follows the law (10). Between 34° and 40° the data can be represented by Eq. (13) and give

$$1/(K_b)^{\frac{1}{2}}=10.3(t-25.7°).$$

The data are not accurate enough to verify the temperature variation of the coefficient of E^2 in Eq. (13). Below 32° we get (from Fig. 12)

$$1/(K_b)^{\frac{1}{2}}=6.9(t-23.6).$$

The variation of $K_b^{-\frac{1}{2}}$ is plotted in Fig. 5 and we notice the similarity with the curve for $1/\kappa_0(T)$. The results below 32° are used in Fig. 12 to verify Eq. (15) and they give

$$R_b=6.9\pm0.2 \quad \text{and} \quad Q_b=150\pm20.$$

More accurate results could be obtained with the large crystal 6. The results in Fig. 13 satisfy again Eq. (15) and give

$$R_c=10.1\pm0.2\,; \quad Q_c=307\pm10.$$

From (16) and (17) follows

$$\rho_b/\rho_c=R_b/Q_b\cdot Q_c/R_c=1.4.$$

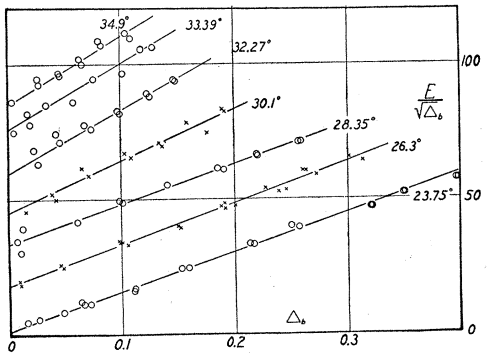

FIG. 12. Verification of Eq. (15).

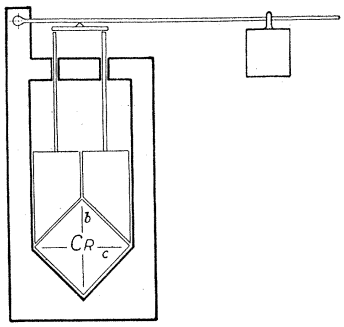

FIG. 14. Device for preventing the piezoelectric deformations. The pressure can be applied to either vertical rod by removing the cross piece.

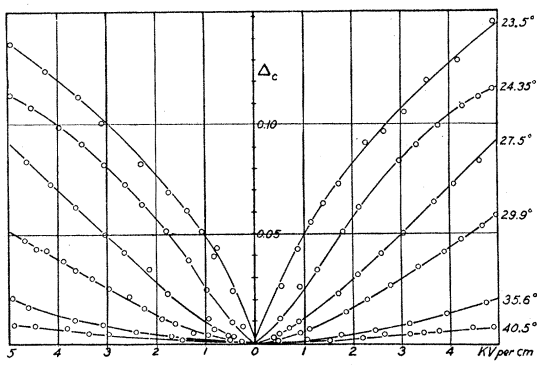

FIG. 13. The Kerr effect above the Curie point for light passing in the c direction (crystal 7).

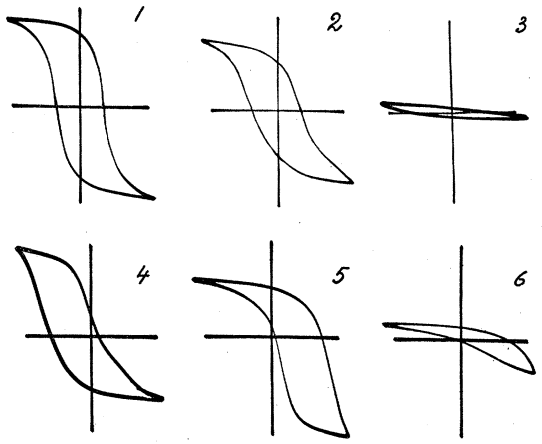

FIG. 15. The change of the hysteresis curve of Rochelle salt with pressure. $t=0°$. (1) Free crystal, (2) pressure 1 kg/cm² on both sides, (3) pressure 7 kg/cm² on both sides, (4) pressure 2 kg/cm² on right side only, (5) pressure 3 kg/cm² on left side, (6) pressure 7 kg/cm² on left side. Maximum field 2 kv/cm.

The observations on different crystals agree therefore with the result $\rho_b/\rho_c=95/70$ found from measurements on the same crystal.

$T < \Theta$

Influence of the piezoelectric back polarization. Four crystals, all of the same cross section $1''\times1''$ and varying in thickness from $\frac{1}{4}''$ to $1''$ were cut with their faces at 45° to the b and c axes, and inserted in the device of Fig. 14. This device permits a pressure to be exerted on the crystal and thus the piezoelectric deformation is partly prevented during either half cycle or the entire cycle of the applied a.c. voltage. The change of the dielectric properties with pressure was investigated with the bridge and the oscillograph. Even the slightest pressure reduces the capacitance of the crystal, when measured with the bridge, to less than 5 percent of its original value. The influence of constraints is particularly interesting in the measurements of the hysteresis loops. Fig. 15 shows that the loop for a "free" crystal is symmetrical, but with the help of pressure we can produce any direction and degree of asymmetry.[21] For very large pressures the loop disappears,[10] but usually the crystal breaks before a photograph can be taken.

These observations lead to the conclusions:

(1) Most investigators[22] have not realized the importance of mechanical constraints. Their asymmetric results are probably produced by the crystal holder.

---

[21] R. David, Helv. Phys. Acta **7**, 647 (1934), reports the same result. This paper appeared after completion of our investigation.

[22] Oplatka, Phys. Zeits. **34**, 296 (1933); references 4 and 6.

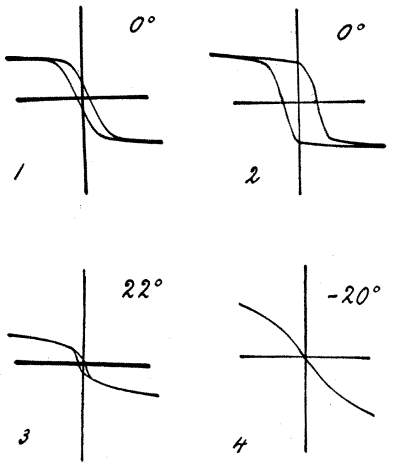

FIG. 16. (1) Hysteresis curve for crystal 3 mm thick at 0°; (2) hysteresis curve for crystal 12 mm thick at 0°; (3) hysteresis curve at 22°; (4) $P(E)$ curve below the lower Curie point.

(2) If the piezoelectric deformation is prevented, the dielectric and all other anomalies disappear. Our theory can explain this. If $\alpha_3=0$, $\Theta=\alpha f T$ is smaller and we get for all temperatures $\Theta<T$. Partial prevention of the piezoelectric deformation reduces Θ and hence shifts the Curie points. This is probably the reason why no two observers find exactly the same values of T_c and T_c'.

(3) The magnitude of the piezoelectric back polarization is determined by y_z and hence depends on the size and shape of the crystal. The elastic problem involved is too complicated to predict a law for this dependence. The hysteresis loop, as was pointed out, depends to a considerable degree on this interaction between polarization and piezoelectric deformation, and hence on size and shape of the crystal.

This dependence is shown in Fig. 16. For thin crystals the hysteresis loop is flat and the remanent polarization is small. Thick crystals give a steep loop[23] and a large remanent polarization.

THE PYROELECTRIC EFFECT

This effect was discovered by Valasek,[4] but it has been questionable[11] whether it is not a false pyroelectric effect. Our results differ considerably from Valasek's, but they leave no doubt that the effect is real and must be considered as due to the temperature variation of the spontaneous polarization. About 30 complete runs, covering the range from $-70°$ to $+40°$ were made. In some runs the temperature was successively increased, in others decreased. Five crystals were tested. All give the same result: Above 25° and below $-18°$ no pyroelectric charges are produced. The effect appears and disappears very suddenly at the Curie points. It is very large and of opposite signs at these temperatures. The reversal of sign occurs near 0°C. Fig. 17 shows the change of the total charge per cm² with temperature. With the same crystal the data are reproducible, but the larger the thickness of the crystal the larger the polarization. The magnitude of the piezoelectric moment is identical with the remanent polarization as measured in the hysteresis loop. The results on all crystals verify at both Curie points the Eq. (21′). The data on crystal 8 give the largest values of P_0. We find from Fig. 17 $h\geqq 1.5\ 10^4$ and at the lower Curie point $h'=2.65\ 10^4$. The maximum moment at 0° is $P_0(O)=600$ e.s.u. Since our observations, Fig. 15 and Fig. 16, show that pressure and the finite thickness of the crystal tend to reduce P_0, and since a crystal is never entirely free, we must expect that these values of h are smaller than their theoretical values.

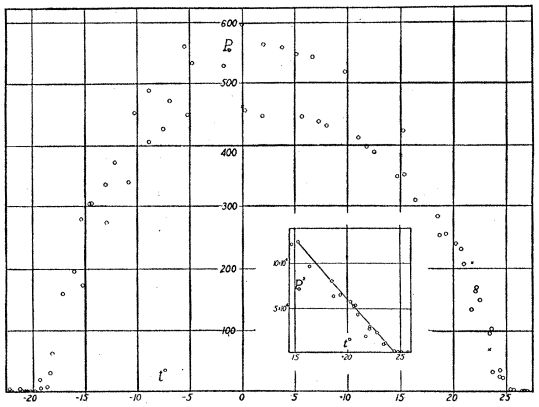

FIG. 17. Pyroelectric effect of Rochelle salt. o total charge per cm² and x remanent polarization of the same crystal.

Further observations of the pyroelectric effect are discussed in a later section.

[23] I. Kurtschatov, Phys. Zeits. d. Sow. **5**, 200 (1934). The forces exerted by the electrodes are perhaps responsible for this effect.

The Kerr Effect of the Spontaneous Field

The temperature dependence of the indices of refraction of Rochelle salt has been measured by Müttrich[24] and Valasek.[4] Both report a linear variation, but Valasek's data are not accurate enough to show the expected effect, and Müttrich's result is based on observation at a few temperatures only.

We have measured the temperature variation of n_c-n_a/λ and n_a-n_b/λ between $-30°$ and $+50°$. The temperature change was performed in the same manner as for the piezoelectric measurements. To satisfy the condition $E=0$ the crystal No. 6 was wrapped in tinfoil with small holes for the passage of light. Each curve in Figs. 18 and 19 is the result of observations at over 100 different temperatures. Above 24° the data can be represented by

$$\begin{aligned}\frac{n_c-n_a}{\lambda}&=-4.159-\frac{S_b}{2.960}+0.0644_6t-0.00040_5t^2,\\ \frac{n_a-n_b}{\lambda}&=6.689+\frac{S_c}{1.384}-0.134t-0.00054_8t^2,\end{aligned}\tag{39}$$

where S_b and S_c are whole numbers. To get agreement with the values of n_a, n_b, n_c given by Valasek we must have

$$S_b=292\pm4;\quad S_c=90\pm2.$$

The curve $(n_b-n_c)/\lambda$ is found by subtraction. Below $-20°$ the change is linear.

$$\begin{aligned}\frac{n_c-n_a}{\lambda}&=-4.392-\frac{S_b}{2.96}+0.0322t,\\ \frac{n_a-n_b}{\lambda}&=6.968+\frac{S_c}{1.384}-0.155t.\end{aligned}\tag{40}$$

At both Curie points the curves show a sharp break. We interpret this as due to the Kerr effect of the spontaneous inner field. Since in all cases the break is in the direction of increasing birefringence, this interpretation is consistent with the observations of the Kerr effect. Extrapolating (39) to temperatures below 24° and extrapolating (40) to temperatures above $-18°$ and calculating the difference between the extrapolated and actual values of $(n_c-n_a)/\lambda$, etc., we get in Fig. 20 the Kerr effect of F_0. In agreement with the fact that $\rho_b>\rho_c$ we find at the upper Curie point $\Delta_0 b>\Delta_0 c$. At the lower Curie point $\Delta_0 b=\Delta_0 c$. This indicates that the longitudinal Kerr effect disappears at lower temperature. Figs. 20 and 21 verify (22′) and give

$$v_b=0.040\pm0.001$$

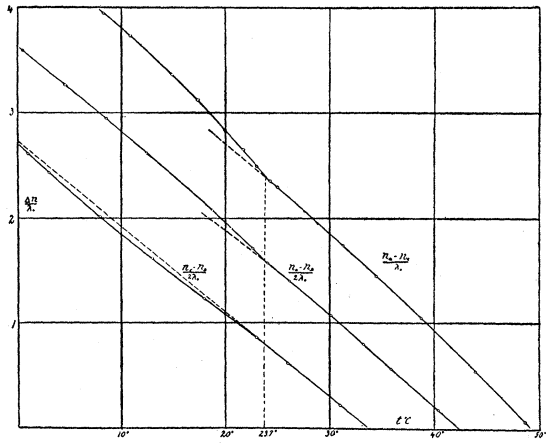

FIG. 18. Temperature dependence of the birefringence of Rochelle salt above 0°.

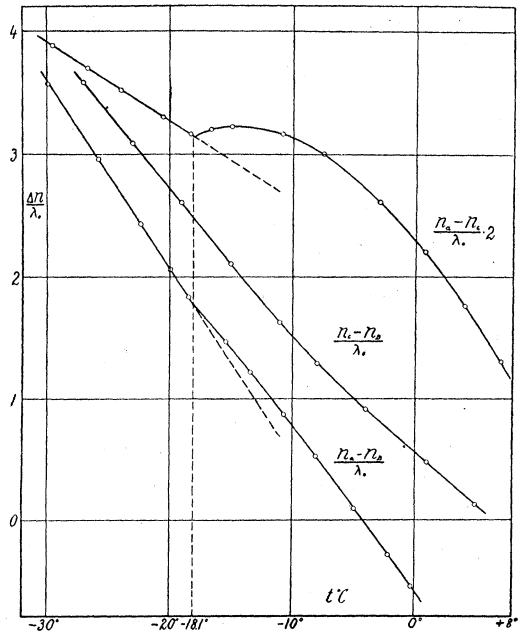

FIG. 19. Temperature dependence of the birefringence of Rochelle salt below 0°.

[24] Müttrich, Pogg. Ann. **121**, 193 (1864).

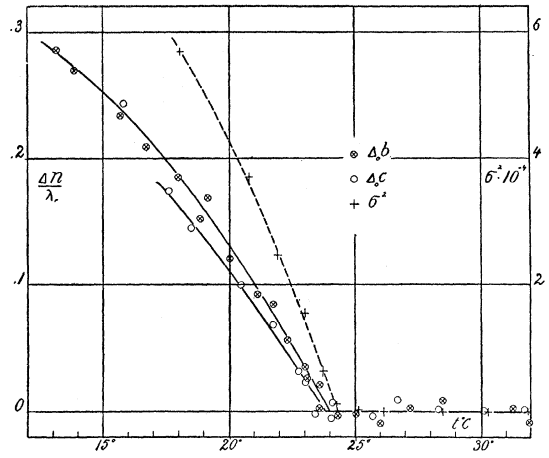

FIG. 20. Kerr effect produced by the spontaneous inner field and pyroelectric moment $\sigma = P_0$ of crystal 6 (measurement with Gaugain's method) near the upper Curie point.

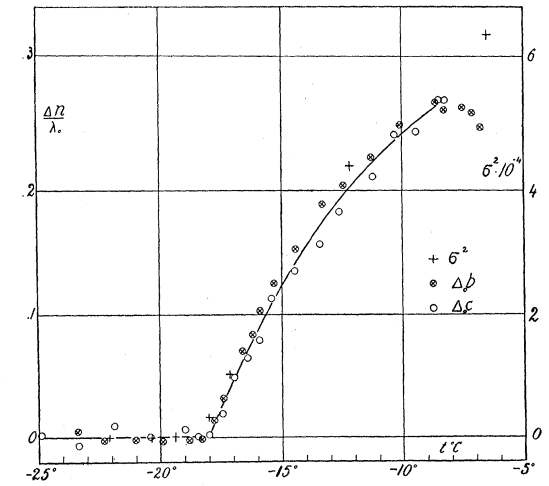

FIG. 21. Kerr effect produced by the spontaneous inner field and pyroelectric moment $\sigma = P_0$ of crystal 6 (Gaugain's method) near the lower Curie point.

and at the lower Curie point

$$v_b' = -0.046.$$

DIELECTRIC MEASUREMENTS

Fig. 5 includes some data of $1/\kappa_0$ for $t < t_c$. The points seem to verify the law (23). They are on a straight line with a slope twice as large as the line for $t > t_c$.

We find that the bridge measurements give for κ_0 the same values as the ones calculated from the slope of the hysteresis loops at the points $E = 0$.

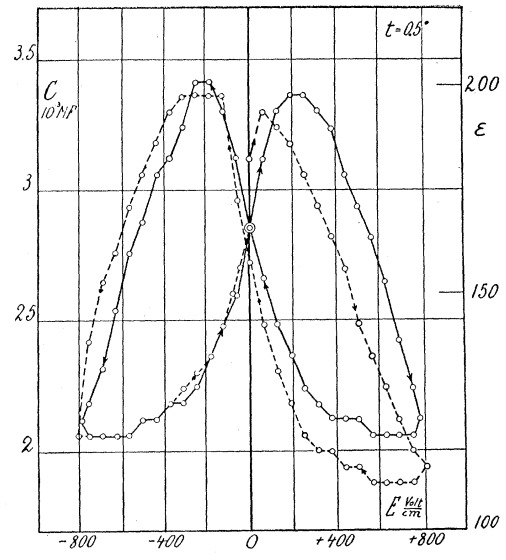

FIG. 22. Variation of the capacitance of Rochelle salt at 0.5° with the electric field. The curve is the derivative of a hysteresis curve.

The existence of the hysteresis loops can also be demonstrated with the help of bridge-measurements with a superposed d.c. field. Fig. 22 evidently represents the derivative dP/dE of a hysteresis curve.

The theoretical value of the coercive field E_c can, for obvious reasons, never be reached. With $g = 1.05$ Eq. (26) gives

$$E_c = (t_c - t)^{\frac{3}{2}} \times 210 \text{ volt/cm}.$$

The experiments (Figs. 16, 22 and 23) give a coercive field of this order of magnitude. E_c increases faster than $(t_c - t)$ but not as fast as $P_0 = h(t_c - t)^2$. Since the conduction of the crystal influences the width of the observed loops no accurate measurements of E_c have been possible. By comparison of loops obtained with 60 and 500 cycle a.c. we are able to approximate the proper compensation for the power loss due to conduction.

THE KERR EFFECT

For small fields a quadratic hysteresis loop is observed (Fig. 23). For large fields, Fig. 24, the effect shows the peculiar behavior predicted by the theory. (Fig. 4.) The initial slope of the curves follows the law 24 and gives ($t_c = 25°$).

$$L_0 = (3.0 \pm 0.1) 10^{-4}.$$

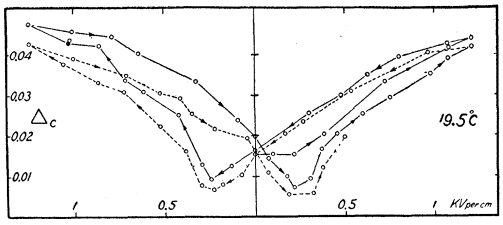

FIG. 23. Hysteresis loop of the Kerr effect (crystal 7).

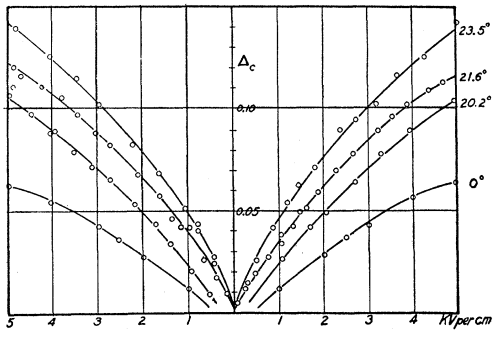

FIG. 24. The Kerr effect of Rochelle salt between the Curie points. c direction, crystal 7.

COMPARISON WITH THE THEORY

The experimental results verify all our theoretical conclusions. It remains only to be shown that the values of the experimental constants are consistent with each other. This is done by testing the six relations (27) to (32).

	Calculated	*Observed*
$g=\left(\frac{M^2}{C}\right)^{\frac{1}{3}}$	$=1.01\pm0.03$	1.05 ± 0.02
$Q_c=\frac{1}{3}\left(\frac{R_c}{g}\right)^3$	$=300\pm30$	307 ± 10
$N=\frac{1}{3}CM$	$=800\pm50$	800 ± 80
$h=9NM$	$=(9.7\pm0.9)10^4$	$>1.5\ 10^4$
$v_b=\frac{R_b}{Q_b}=1.4\frac{R_c}{Q_c}$	$=(4.6\pm0.5)10^{-2}$	$(4.0\pm0.1)10^{-2}$
$L_c=\frac{1}{R_cQ_c}$	$=(3.2\pm0.2)10^{-4}$	$(3.0\pm0.1)10^{-4}$.

For the quantities related to the behavior above the Curie point the agreement is excellent. For the quantities related to the "ferro" dielectric properties the theory gives values of the correct order of magnitude. From (33), (34) and (35) we get

$$f\gamma=1.67\pm0.006,$$

$$\beta f^4=(5.8\pm0.7)10^{-8},$$

$$\rho_c f^2=(4.7\pm1.0)10^{-8}.$$

These values hold for the upper Curie point. From the definition (8) follows $\gamma<1$. Hence the factor f is of the same order of magnitude, as Lorentz's factor $4\pi/3$. We are not facing the difficulties encountered in Weiss's theory of ferromagnetism. If the cubic term in (7) is interpreted with the help of the theory of dipoles, it is easy to show that βf^4 should be of the above order of magnitude.

The constant ρ shall be compared with the Kerr constant of liquids. For normal liquids the Kerr constant K is about 5×10^{-8} and we have

$$\rho=K[3/(\epsilon+2)]^2.$$

Hence for liquids ρ has the same order of magnitude as K, while for Rochelle salt the largest value of ρ is smaller than 10^{-8}. The quadratic electro-optical effect of Rochelle salt can therefore be considered to be a real Kerr effect. The large magnitude of this and all other effects is not due to an anomalous structure of the crystal or abnormal properties of the molecules. They are due to the electric interaction between the molecules, which produces a very large inner field F under the influence of a small outer field.

BARKHAUSEN EFFECT AND WEISS REGIONS

The theory of ferromagnetism leads to the existence of a pyromagnetic effect for iron. This effect, which is analogous to the pyroelectric effect of Rochelle salt, has never been observed, and this has led to the conclusion that a block of iron consists of a large number of elementary magnetic regions. The existence of the pyroelectric effect in Rochelle salt indicates therefore that here a small crystal represents a single "Weiss region."[25] The directions of "easy polarization" are the $+a$ and $-a$ directions. Theoretically the pyroelectric moment could reverse its direction. Such a reversal has never been observed, even when the crystal was cooled while it was under the influence of an electric field of 1000 volt/cm. The direction of P_0 seems

[25] Or there may be a large number of elementary regions but most of them are polarized in the same direction. This would explain why we get much better agreement for L_c and v_c than we get for h.

to be determined by some small internal asymmetries, as for instance, small internal stresses which have not been removed by annealing. In accordance with the hypothesis of a single Weiss region no Barkhausen discontinuities could be observed for small crystals.

This hypothesis raises two questions, namely: (a) Why are the Weiss regions in Rochelle salt much larger than in ferromagnetism? and (b) how large may a crystal be to represent only a single region?

To question (a) we propose the following answer: Because there exists electric but no magnetic conduction. In magnetism a spontaneous polarized region produces an outer magnetic field which causes the neighboring regions to become polarized in the opposite direction. In Rochelle salt this effect does not exist because the free charges on the surface of a region are quickly neutralized by conduction.

In order to answer question (b) three large crystals with cross sections between 10 and 50 cm^2 were investigated. The observations indicate that such large crystals contain a large number of oppositely polarized Weiss regions.[26] The evidence is not conclusive, but interesting enough to be reported.

The previously discussed method shows a very small, and sometimes no pyroelectric effect for large crystals.

The existence of a Barkhausen effect was demonstrated in two ways: The electric field in the crystal was slowly and continuously increased with the help of an induction regulator in the primary of the kenotron outfit. In series with the crystal was an induction coil. A second coil, loosely coupled to the first, was connected to an audiofrequency amplifier feeding a loudspeaker. In the voltage range which corresponds to the steep part of the hysteresis loop a large number of sharp clicks could be heard. A thyratron operated counter recorded between 70 and 120 discontinuities for crystal 7. No such discontinuities occur in the saturation range, and they disappear for temperatures above the Curie point.

The oscillograph gave for these crystals a rapidly and irregularly flickering line in the steep part of the loops. This flickering, however, disappeared after about five minutes of continuous operation, and could only again be obtained after giving the crystal a rest for several hours. With 500 cycle a.c. the phenomenon continues for a longer time, and by applying alternately 500 cycle and 60 cycle a.c. for 3 minutes, the flicker phenomenon continued to appear for two hours. We have no explanation for this curious behavior. Successful attempts were made to observe directly the existence of many Weiss regions in large crystals. The well-known method of demonstrating pyroelectricity with electrically charged powders is also successful for showing the pyroelectric effect of Rochelle salt. Best results are obtained by heating the crystal from $-30°$ to $0°$ and using Bürker's[27] mixture of sulphur, lycopodium and carmine. The pair of faces of small crystals, which is normal to the a axis, appears brightly colored, one face red, the other yellow. For large crystals, however, each face shows a system of red and yellow patches, occasionally arranged in a regular checkered pattern, red and yellow spots alternating about 2 to 3 cm apart and arranged in lines at 45° to the b and c axes. Usually however the pattern is quite irregular and further work is required before any conclusion can be drawn.

Conclusion

The experiments verify the proposed theory within the limits of experimental errors. Measurements near the lower Curie point, where the conductivity is negligible, would furnish more accurate data. The measurements give values of f, γ, β and ρ which are of the correct order of magnitude. They give only the product $f\gamma$ and it is not possible to calculate f and $\Theta(T)$ without introducing a further assumption.

This new assumption is based on the fact that the Curie-Weiss law (37) is satisfied with excellent precision for all temperatures above 34°. The analogy with the corresponding law in ferro- and paramagnetism suggests that above 34° Θ is constant. We emphasize that this assumption is arbitrary and may have to be changed. From it follows $\Theta = T_1$ for $t > 34°$ and

[26] Results which support this conclusion have been reported by Kurtschatov, Phys. Zeits. d. Sow. **4**, 125 (1933).

[27] K. Bürker, Ann. d. Physik **1**, 474 (1900).

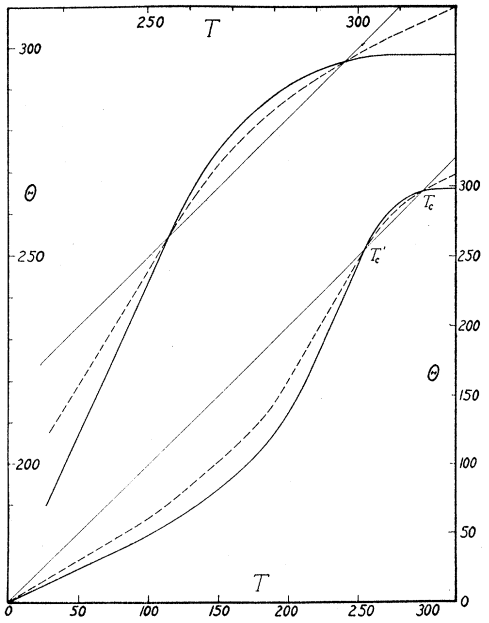

FIG. 25. Change of the Curie temperature Θ with temperature, assuming $f=2.19$, and for $f=4\pi/3$.

hence

$$f=T_1/c_1=2.19\pm0.01.$$

With the help of (37) and the values of c_i and T_i we are now able to construct the curve $\Theta(T)$ given in Fig. 25. Between the Curie points $\Theta(T)$ is calculated from the data on P_0 and Δ_0. The dotted curve corresponds to the assumption $f=4\pi/3$ but the assumption $f<4\pi/3$ is not inconsistent with any observation.

With the help of this curve and the values of β and ρ we can calculate all our experimental results. From it follows the value of the inner field. The magnitude of the spontaneous inner field at 0° for instance is found to be 0.77 10^6 volt/cm.

This paper is an attempt to explain the anomalous properties of Rochelle salt without making any assumptions concerning the molecular mechanism involved. It gives the fundamental relations on which an atomistic theory can be based.